

## Chapter 13

# Modeling and Forecasting Systems for Fusarium Head Blight and Deoxynivalenol Content in Wheat in Argentina

Ricardo C. Moschini, Malvina I. Martínez, and María Gabriela Sepulcri

**Abstract** In Argentina, wheat Fusarium Head Blight (FHB) is predominantly caused by *Fusarium graminearum*, being deoxynivalenol (DON) the main associated mycotoxin. The sporadic weather-induced nature of FHB in the Pampas region led to the development of weather-based disease and DON forecasting systems. Infective events were identified by head wetting resulting from synchronic occurrence of precipitation and high relative humidity, around wheat anthesis. Retrospective model predictions were able to identify synoptic situations and meteorological predictors of increasing space-temporal scale (for developing specific short-range and seasonal weather forecasts), regarding the disease. In the north-eastern quadrant of the Pampas region, greater disease levels were expected with greater August Southern Annular Mode values and dominance of meridional north-northeastern atmospheric circulation in September. In the southern, the Southern Oscillation index and variables associated to blocking action situations in the south (October), strongly helped to explain disease variability. Climate change impact was assessed retrospectively analyzing the trend lines of FHB incidence predictions (1931–2010), which showed light positive slopes, larger towards southern Pampas region. Prospectively, the anomaly map resulting from the difference between disease incidence estimated by future meteorological data (2071–2100, A2 scenario) and baseline climate (1961–1990), presented positive deviations in the southern Pampas region. The spatial distribution of model-based FHB incidence values using only land weather station network data was compared satisfactorily with those using both land and satellite data. Conclusions derived from FHB forecasting systems and specific weather forecasts are being used to assist producers in disease control measures to be employed.

---

R.C. Moschini (✉) • M.I. Martínez • M.G. Sepulcri  
Instituto de Clima y Agua (CIRN), Instituto Nacional de Tecnología Agropecuaria (INTA),  
Los Reseros y Las Cabañas s/n, B1712WAA Hurlingham, Argentina  
e-mail: rmoschini@cnia.inta.gov.ar; mmartinez@cnia.inta.gov.ar; gsepulcri@cnia.inta.gov.ar

## 13.1 Introduction

Fusarium Head Blight (FHB) is a disease caused by several *Fusarium* species. In Argentina, 90 % of the pathogens isolated from blighted heads were *Fusarium graminearum* Schwabe [teleomorph *Gibberella zeae* (Schwein.) Petch] (Carranza et al. 2002), which produces exclusively the mycotoxins deoxynivalenol (DON) and zearalenone (Faifer et al. 1992).

Argentinean wheat cropping area is very extensive (4.63 million hectares in 2011–2012 growing season), distributed in five provinces of the Pampas region with different ecological conditions (Buenos Aires, Córdoba, Santa Fe, Entre Ríos and La Pampa). Therefore, no wheat FHB epidemic has ever covered the whole area in a given time. The worst FHB outbreaks occurred in the north-eastern quadrant of the Pampas region, producing wheat yield losses that ranged from 10 to 30 % in 1978. Favorable meteorological conditions once again prevailed in 1985, 1993 and 2001, enhancing FHB infections and causing significant wheat losses. In the south-eastern portion of wheat growing region, the main durum wheat (*Triticum durum* Desf.) area, severe epidemics occurred in 1963, 1976, 1978 and 1985, with crop losses as high as 70 % (Moschini et al. 2004).

The sporadic nature of FHB, strongly related to weather factors, led to development-validation of empirical and fundamental-empirical forecasting systems in the Pampas region. Also, from controlled-environment studies, a forecasting system of DON content in wheat mature grain was developed. Retrospective FHB model predictions were able to make maps showing their regional climate potential and to carry out studies to identify synoptic situations and meteorological predictors of increasing spatial-time scales regarding the pathosystem. A new empirical model for predicting FHB incidence where relative humidity was replaced by thermal amplitude was used to study the effect of climate change retrospectively and by comparing the recent past (1961–1990) and future (2071–2100) climate. All this knowledge is being used for assessing FHB risk and its spatial distribution (supported by land and remote sensing data) in the Pampas region before wheat harvest.

## 13.2 Development of Weather-Based Fusarium Head Blight/Deoxynivalenol Forecasting Systems

### 13.2.1 Development of Weather-Based Fusarium Head Blight Forecasting Systems

#### 13.2.1.1 Empirical Approach

Applying linear regression techniques, different models up to a maximum of three independent meteorological variables were fitted to FHB incidence (*I* %) data in Pergamino (north-eastern of Buenos Aires province) (Moschini and Fortugno 1996). Annual mean percent disease incidence computed from values recorded for wheat

cultivars grouped by their similar heading dates were used to fit the models. Using daily records of maximum ( $xT$ ) and minimum ( $nT$ ) temperature, precipitation ( $Pr$ ) and relative humidity ( $RH$ : average of the 0800, 1,400 and 2,000 h observations) obtained from a standard weather station, independent meteorological variables were calculated. Daily average temperature ( $Td$ ) was calculated as half the sum of the daily minimum and maximum temperatures. The closest associations between environmental variables and FHB incidence data were obtained in a time period beginning 8 days prior to heading date (when 50 % of the heads were fully emerged: emergence of first heads) and ending when 530 degree days ( $DD$ ) were accumulated (base temperature: 0 °C). This period was regarded as the susceptible period for infection ( $SPI$ ) lasted 26–32 days in this study.

Variable  $NP$  (number of 2-day periods with  $Pr \geq 0.2$  mm) and  $RH > 81$  % during the first day and  $RH \geq 78$  % during the second one) showed the strongest association with disease incidence ( $R^2 = 0.81$ ). Long anther wetness periods (48–60 h) favor the infection of the pathogen. Not having duration measurements of precipitation-induced wetness events, their potential lengths were better considered by combining the occurrence of precipitation with high air relative humidity records in a 2-day window. A low correlation was found between precipitation frequency and disease incidence ( $R^2 = 0.17$ ). The Eq. (13.1) was finally selected for predicting FHB incidence ( $PI$  %).

$$PI\% = 20.37 + 8.63 NP - 0.49 nDD \quad R^2 = 0.86 \quad (13.1)$$

in which  $nDD$  represents the daily accumulation of the residuals resulting from subtracting 9 to the  $nT$  values ( $< 9$  °C) and the exceeding amounts of  $xT$  from 26 °C. This equation was adjusted and validated for northern locations than Pergamino (Moschini et al. 2001). For southern areas of the Pampas region (Moschini et al. 2004; Carranza et al. 2007), lower and upper temperature thresholds were changed by 11 and 30 °C and the  $SPI$  was fit in 450  $DD$ . With the same data, Moschini et al. (2008) developed another FHB incidence predicted model that only requires daily data of maximum and minimum temperature and precipitation to calculate its variables (Eq. 13.2).

$$PI\% = -9.15 + 6.47 ND + 0.35 pDD \quad R^2 = 0.81 \quad (13.2)$$

being  $ND$ : number of days with simultaneous occurrence of  $Pr$  and thermal amplitude ( $TA = xT - nT$ )  $< 7$  °C;  $pDD$ : results of accumulating residuals  $> 9$  °C in  $nT$ , in those days where  $xT$  and  $nT$  are  $< 25$  °C and  $\geq 9$  °C, respectively.

### 13.2.1.2 Fundamental-Empirical Approach

From 84 FHB incidence ( $I$  %: percentage of diseased heads) and severity ( $S$  %: percentage of diseased spikelets in the diseased heads) values registered in commercial wheat cultivars (susceptible and moderately susceptible) at Pergamino and M. Juárez (south-eastern Córdoba province) (ten growing seasons), observed

*Fusarium* index ( $FI \% = I \% * S \% / 100$ ) values were calculated and satisfactorily contrasted with predicted ones using a fundamental-empirical approach (Moschini et al. 2002).

**Predicted *Fusarium* index (PFI %)** values were obtained following the next steps:

- (a) Daily progress of anthesis (% of wheat heads with exposed anthers): from field observations in a single wheat cultivar, a polynomial function between the logit of the proportion of head with anthers (Anther, values from 0 to 1) and the time in degree days ( $DD_{12}$ : daily accumulation of  $Td \geq 12$  °C) was fit.

$$\begin{aligned} \text{LogitAnther} = & -6,765052912 + 0,136395967 DD_{12} - 0,000694621 DD_{12}^2 \\ & + 0,000001384 DD_{12}^3 - 0,000000001 DD_{12}^4 \end{aligned} \quad (13.3)$$

where LogitAnther is the natural logarithm of (Anther/1-Anther);  $DD_{12}^2 = DD_{12} * DD_{12}$ ;  $DD_{12}^3 = DD_{12} * DD_{12}^2$ ;  $DD_{12}^4 = DD_{12} * DD_{12}^3$ . Solving [Exp(LogitAnther)/(1+Exp(LogitAnther))]\*100, the daily percentage of heads with anthers were obtained. The *SPI* began 4 days prior the observed heading date and finished when 530 *DD* were accumulated.

- (b) Predicted severity (*PS* %): in controlled environment, Andersen (1948) established the percentage of infection in wheat heads inoculated with *Fusarium graminearum* conidia, exposed to different wetness periods (*W*: from 18 to 72 h) and temperatures during wetness periods ( $T_w = 15, 20, 25$  and  $30$  °C). A polynomial function was fit between the logit of the severity (*S*, values from 0 to 1) and *W* (h) and  $T_w$  (°C), like individual and interactive effects.

$$\begin{aligned} \text{LogitS} = & 38,77166158 - 0,53815698 W - 6,02985565 T_w + 0,26849793 T_w^2 \\ & - 0,00396097 T_w^3 + 0,04990941 I_1 - 0,00092343 I_2 \end{aligned} \quad (13.4)$$

where LogitS is the natural logarithm of (S/1-S);  $T_w^2 = T_w * T_w$ ;  $T_w^3 = T_w^2 * T_w$ ;  $I_1 = T_w * W$ ;  $I_2 = T_w^2 * W$ . *PS* % values were obtained solving [Exp(LogitS)/(1+Exp(LogitS))]\*100.

In order to use Eq. (13.4), **equivalence rules** defining *W* and  $T_w$  from daily Pr, xT, nT and RH registered at standard weather stations, were established. Using criteria derived from the empirical approach, it was defined that: 1 day with Pr ( $\geq 0.2$  mm) and RH  $\geq 81$  % is equal to  $W=24$  h; two consecutive days with Pr and RH  $\geq 81$  % is equal to  $W=48$  h; three consecutive days with Pr and RH  $\geq 81$  % is equal to  $W=72$  h. A maximum *W* period of 72 h was analyzed. If prior and/or after *W* period of 24 and 48 h, Pr and RH  $\leq 77$  % are registered, 3 h of wet are added. If Pr and RH  $>77$  % and  $<81$  % (prior and/or after) are registered, 6 h of wet are added. Occurrence of RH  $>77$  % and  $<81$  % after *W* periods, 3 h are added. The temperature during the wet period ( $T_w$ ) resulted of averaging the mean daily temperatures (Td), weighted for the wet duration in each day involved. If  $T_w$  is  $<15$  °C, severity values are only calculated for wet periods  $\geq 48$  h.

- (c) The final **PFI** % value resulted from adding the partial products between (a) and (b) (divided by 100), calculated for all the wet periods found throughout the wheat **SPI**. As a consequence of validation studies, just a few small changes of the original methodology were made. The SPI lasted 450 **DD**<sub>10</sub> (daily accumulation of  $T_d \geq 10^\circ\text{C}$ ) in southern Pampas region (Moschini et al. 2004; Carranza et al. 2007) and also an upper daily mean temperature threshold (If  $T_d > 20^\circ\text{C}$  then  $T_d = 20^\circ\text{C}$ ) during days with precipitations was included (Moschini et al. 2012).

### 13.2.2 Development of Weather-Based Deoxynivalenol Content Forecasting System

Environment-controlled experiments were conducted in Castelar (northeastern Buenos Aires province) in 2006 and 2007 to study the effect of wetness duration (**W**) and temperature ( $T_w$ ) on three visual estimates of FHB (**I** %, **S** %, **FI** %) and grain DON content, and to develop a weather-based forecasting system of the mycotoxin (Martinez et al. 2012). Artificial inoculation with toxicogenic local *Fusarium graminearum* strains was used. Both **FI** % and **S** % were significantly related to **W** and  $T_w$  and strongly associated to DON content ( $R^2=0.66$  and  $0.73$ , respectively). Relationships between environmental factors and DON content were not significant. The  $T_w$  and **W** treatments allowed to establish three important thresholds. The first was  $9.5^\circ\text{C}$ , at which there were no FHB symptoms, the second was  $15^\circ\text{C}$ , at which both **S** % and **FI** % increased when **W** increased and the third was around  $20^\circ\text{C}$ , at which **S** % and **FI** % had less response to **W**. Symptom expressions started around  $14^\circ\text{C}$  for all **W**, producing different **S** % levels ( $5.5$ – $24.3$  %). In a similar experiment with *F. graminearum* and environmental-controlled conditions, Andersen (1948) did not find **S** % levels higher than  $1.5$  % at  $15^\circ\text{C}$ . Differences in the adaptation of pathogen strains to the place of origin could explain the differences between both studies. Coincidentally, Zoldan (2008) observed low disease levels in wheat spikes inoculated with local *F. graminearum* isolates (southern Brazil) at  $10^\circ\text{C}$ , concluding that the pathogen is adapting to lower temperatures and is more aggressive.

From the information generated by the environment-controlled experiments from Martinez et al. (2012), it was possible to modify the earlier explained fundamental-empirical forecasting systems of *Fusarium* index (Moschini et al. 2002) as well as to predict DON content. As first step, the next polynomial equation (Eq. 13.5) was adjusted between the logit of FHB severity (**S**, from 0 to 1) and the different chamber treatments (**W** and  $T_w$ ) ( $R^2=0.96$ ):

$$\begin{aligned} \text{LogitS} = & -52.68809110 + 0.03705345 W + 8.17557456 T_w \\ & - 0.45642424 T_w^2 + 0.00856901 T_w^3 \end{aligned} \quad (13.5)$$

being LogitS: natural logarithm of  $(S/1-S)$ ;  $T_w^2 = T_w * T_w$ ;  $T_w^3 = T_w^2 * T_w$ . Solving  $[\text{Exp}(\text{LogitS})/(1 + \text{Exp}(\text{LogitS}))]*100$ , **PS** % values were found. After incorporating Eq. (13.5) into Moschini et al. (2002) forecasting system, 82 predicted *Fusarium* index (**PFI**%) values were obtained and regressed against field observed ones (Eq. 13.6;  $R^2=0.54$ ).

$$\mathbf{PFI}_f\% = -4.0089 + 0.4351 \mathbf{PFI}\% \quad (13.6)$$

being  $\mathbf{PFI}_f\%$  the predicted *Fusarium* index values adjusted to field conditions. Finally, a linear regression was fit between DON grain content and observed *Fusarium* index (**FI**%) values (37 pair values resulting from chamber treatments). Under the assumption that in field conditions low FHB intensity leads to low DON contamination, the regression line was corrected to zero intercept. The determination coefficient ( $R^2$ ) was 0.66 and the equation was the following:

$$\mathbf{DON}(\text{mg} / \text{Kg}) = 57.865 \mathbf{FI}\% \quad (13.7)$$

The new forecasting system developed was run for each cultivar with its flowering date and daily meteorological data from Oliveros (Santa Fe province), for the 2007 wheat growing season. Twelve  $\mathbf{PFI}_f\%$  values were obtained and adjusted to field conditions (Eq. 13.6). Using Eq. (13.7), 12 DON values were estimated. The *t*-test determined no significant differences between mean observed **FI**% and  $\mathbf{PFI}_f\%$  and DON values.

Unlike the results from Martinez et al. (2012), other studies found significant relationships between the environment and grain DON content (Xu et al. 2007; Hooker et al. 2002; Lacey et al. 1999). Varying degrees of association between FHB intensity and DON accumulation in harvested grain, including high positive, low, and negative correlations, as well as correlations close to zero, have been reported (Paul et al. 2005). According to Snijders and Kretching (1992) the mycotoxin can be translocated from floral tissues to the grain, and considering that *F. graminearum* may colonize the floral and grain tissues (Xu et al. 2007), the symptoms on the floral tissues may be relevant for estimating DON content. Using meta-analysis of transformed correlations of published and unpublished studies on the relation between FHB visual intensity measures and DON content, Paul et al. (2005) concluded that the *Fusarium* index had a significantly higher correlation with DON than either incidence or severity. According to Paul et al. (2005), between 27 and 53 % of the variation in DON content is explained by the variation in disease intensity. Other factors may influence DON content and interfere in the precision of the estimation. It is essential to continue collecting samples of wheat grains under field conditions, with the respective disease information to strengthen the reliability of several relationships, for example Eq. (13.7), which relates **FI**% with DON. The inclusion of field data may increase the variability of values and thus make the proposed system more possible to extrapolate.

## **13.3 Applications of Fusarium Head Blight Forecasting Systems**

### ***13.3.1 Climate Risk of the Pampas Region Regarding Fusarium Index***

For 37 stations of the Pampas region with daily meteorological data for 1971–2011 time series, levels of *Fusarium* index for each year were estimated by the fundamental-empirical forecasting system (Moschini et al. 2012). The probability of occurrence of severe *Fusarium* index (considered here as PFI % > 10) was calculated for each station. The spatial distribution of these probabilities for the Pampas region can be observed in Fig. 13.1. Northeastern quadrant of the region shows the highest probability of severe attacks (four to six severe epidemics out of 20 years). Towards the southern, the disease gradually decreases, expecting two to three severe outbreaks out of 20 years in the southeastern of the region. The minimum climate risk of the region regarding the disease is observed in the southwestern quadrant.

### ***13.3.2 Development of Specific Fusarium Head Blight Short Range Meteorological Forecasts***

Many weather-based forecasting systems in plant pathology estimate epidemic risk in order to make sound disease management decisions, reaching their maximum potential in areas where weather conditions sporadically favor epidemics, unlike those areas in which conducive conditions always prevail. Numerous disease forecasting systems recommend post-infection chemical control after identifying favorable weather events, when contact fungicides are ineffective against already established infections. Past weather patterns are analyzed instead of analyzing present and future weather conditions. Only a few disease predictive systems have incorporated short range meteorological forecasts for truly predicting the infection (Vincelli and Lorbeer 1988; Raposo et al. 1993; Baker and Kirk 2007). Bourke (1970) pointed out the potential value of analyzing the conducive weather factors for infection and identifying the types of recurrent meteorological situations over synoptic weather charts (surface and higher levels; actual and forecast), complementing the role played by simple disease predictive models.

FHB infection events depend strongly on the occurrence of both precipitation-induced long wetness periods (24–72 h) and warm temperatures around wheat flowering. Little time after infection is available for effective triazole fungicide applications (1 or 2 days). Therefore both, FHB weather-based forecasting systems and specific short range meteorological forecasts can help farmers assess

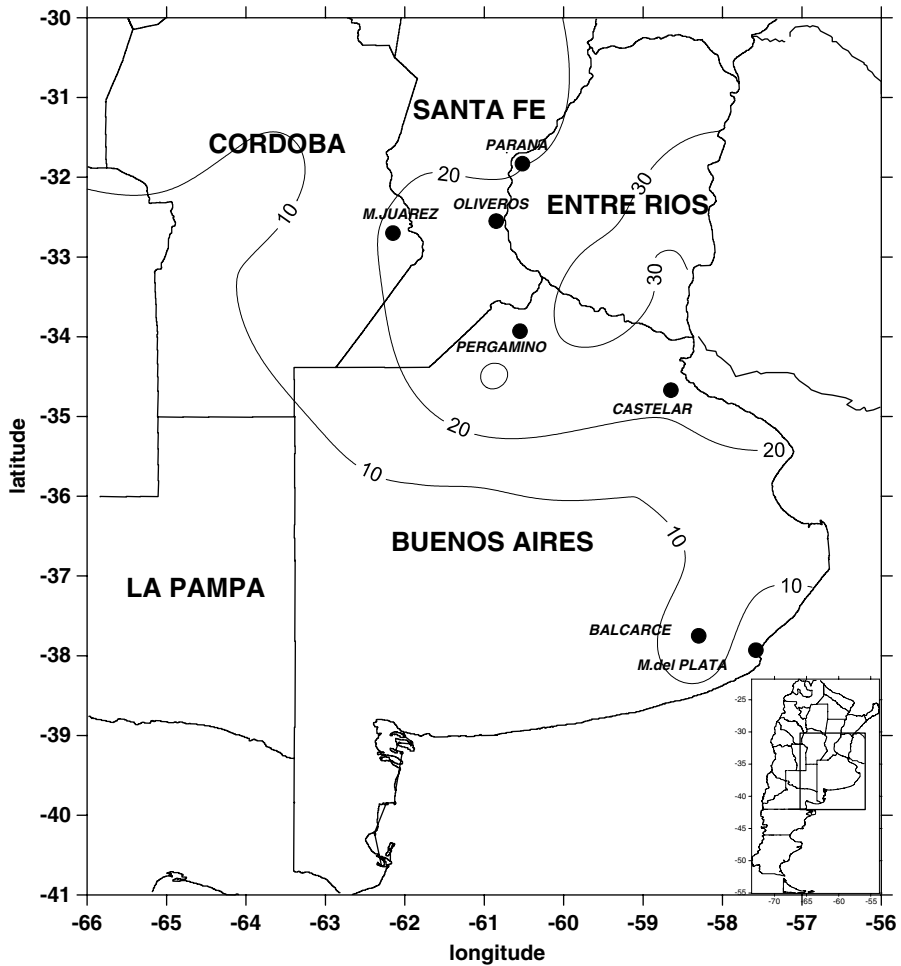


**Fig. 13.1** Percentage of years with a severe level of *Fusarium* index (PFI > 10 %) predicted by the fundamental-empirical forecasting system (1971–2011 series; 37 meteorological stations) in the Pampas region (Córdoba, Santa Fé, Entre Ríos, La Pampa and Buenos Aires provinces)

the risk of FHB infection when deciding whether to apply a fungicide. For this goal, studies were carried out for characterizing types of atmospheric circulation at synoptic scale associated to the occurrence of FHB infection events. From Alessandro (2003) studies about the influence of blocking action anticyclones in the south of South America on temperature and precipitation in the Argentinean territory, the effect of this synoptic phenomenon was analyzed in relation to FHB epidemics. Results derived from these researches may be useful for the interpretation of available short range weather forecasts (1–5 days), making them specific for the disease.

### 13.3.2.1 Synoptic Weather Patterns Related to Fusarium Head Blight Infection Events

Synoptic weather patterns associated to FHB infection events in several sites of the Pampas region were characterized (Moschini 2011). Infection events were identified by head wetting resulting from synchronic occurrence of precipitation and high relative humidity, around wheat anthesis. FHB infection event severities were estimated by Eq. 13.4 (fundamental-empirical approach) in five sites (eastern Pampas region) throughout 45-day periods (in which wheat head with anthers could be available) for the 1971–2006 wheat growing seasons. Predicted FHB severities were categorized into levels: severe ( $PS \% > 3.7$ , percentile 75 %), moderate ( $PS \% \leq 3.7$  and  $> 1$ ), light ( $PS \% \leq 1$ , percentile 25 %). In Paraná (western Entre Ríos province), 51 and 27 FHB infection events were identified as severe and light respectively, including their initial day. From NCEP/NCAR reanalysis (Kalnay et al. 1996), 3-day sequences (initial day and the two previous) of mean daily 1,000 hPa geopotential height (gph) maps were obtained for South America. Using the technique developed by Lund (1963), each 3-day sequence of mean daily 1,000 hPa gph map was correlated ( $r$ : Pearson correlation coefficient) with all the other 3-day sequences analyzed. In Paraná, one 3-day sequence map (initial day infection event: 12 October 1993) had the most  $r \geq 0.70$  (33 out of 51). The same process was carried out for 27 light infection events. In this case, one 3-day sequence map (initial day: 16 September 1982) had the most  $r \geq 0.70$  (14 out of 27). Figure 13.2 shows both synoptic patterns, resulting of averaging (point by point of the 1,000 hPa gph grid) the 33 (severe infections) and 14 (light infections) 3-day sequence maps. The mean synoptic pattern related to severe FHB infection events (Fig. 13.2, left) presented a low pressure centre located central-north of Argentina, involving ascendant air inducing precipitations (primary source of wetness periods required for FHB infection events). When the 3-day sequence (initial day and the two previous) of gph at 1,000 hPa was analyzed, two strong anticyclones (Pacific and Atlantic) and a low pressure axis over Argentina was characteristic. The strong Atlantic high pressure centre produced advection of warm and humid air during the two previous days to the beginning of FHB infection episodes. The mean synoptic pattern associated to light FHB events (Fig. 13.2, right) showed a latitudinal high pressure axis and two low pressure areas, one strong over central northern Argentina and the other southern. A weakening in the south Atlantic anticyclone activity decreased the incoming of northern air masses. The strong Pacific anticyclone circulation shifted rapidly the continental cyclone to the north of Argentina. This fast displacement of the low pressure area might explain the occurrence of shorter periods of wetness (precipitation-induced) related to light FHB infection events.

### 13.3.2.2 Influence of Blocking Action Situations in the Southern of South America on Fusarium Head Blight Infection Events

From daily data of maximum and minimum temperature, precipitation and relative humidity, annual model-based *Fusarium* index (fundamental-empirical approach) values were estimated (1971–2006), throughout the susceptible period for infection

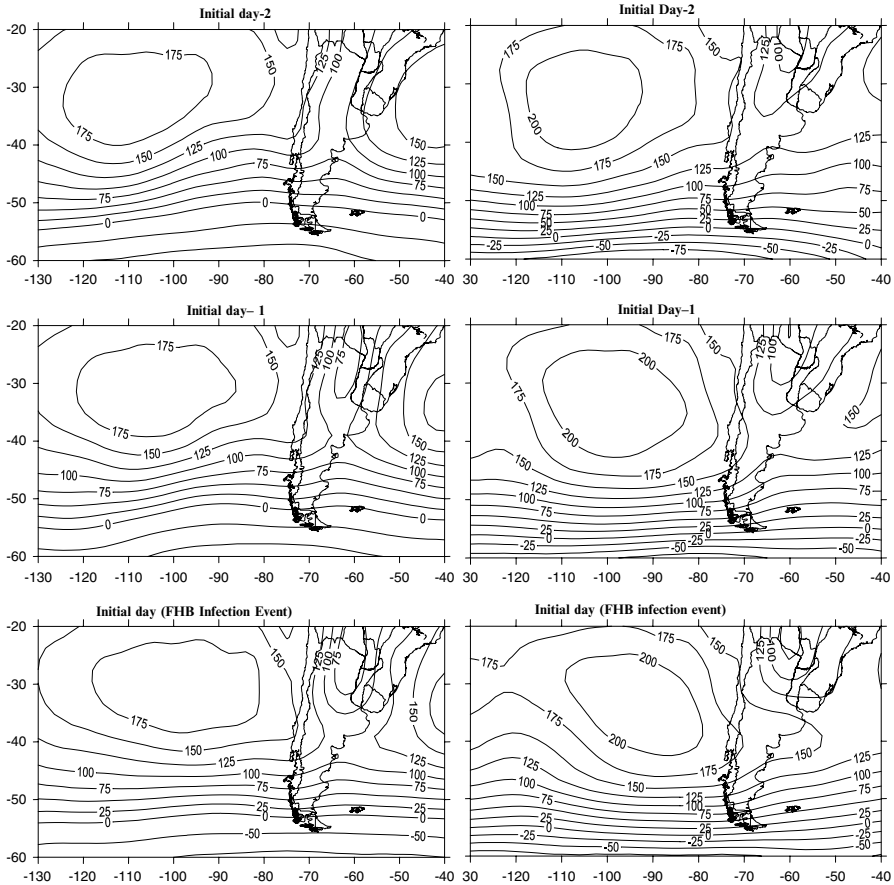


**Fig. 13.2** Mean synoptic weather patterns related to severe (*left*) and light (*right*) FHB infection events

(SPI) in Paraná, Pergamino and Balcarce (Fig. 13.1) (Moschini 2011). Combining precipitation occurrence and relative humidity threshold values, wetness periods or infection events (24–72 h) were identified. A zonal index (ZI) was calculated for 100°, 70° y 40°W longitudes, throughout the SPI.  $ZI = U(30^{\circ}S) + U(60^{\circ}S) - 2U(45^{\circ}S)$ , where  $U$  is the wind zonal component (m/s) in 500 hPa. Positive values of ZI indicate weaker westerly Patagonia winds at 45°S latitude. The highest mean percentage of days coincident with FHB infective events (69.7 %) observing  $ZI > 0$ , was reached by the zonal index calculated in 70°W. A greater frequency of days with  $ZI > 0$  values was observed accompanying the occurrence of FHB infective events of longer duration ( $\geq 30$  h), especially in Balcarce. More persistent blocking action situations (5 or more days with  $ZI > 0$ ) were registered more frequently in

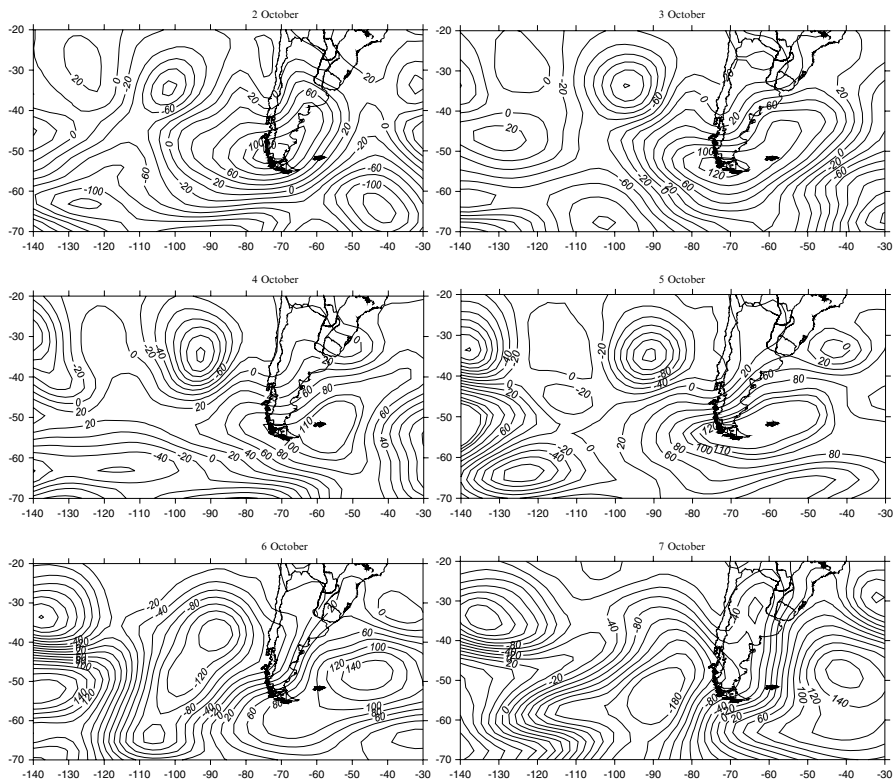


**Fig. 13.3** Six day-sequence (2 October to 7 October) of anomaly maps of geopotential height at the level of 1,000 hPa, along the blocking action situation at 70°W observed at the southern South America in 1978 (severe FHB epidemic in the northeastern Pampas region quadrant)

severe annual epidemic cycles, especially in southern Pampas region. For the most severe FHB epidemics (observed and predicted by models) in the Pampas region, 55–100 % of days with occurrence of infective events in the SPI observed positive values of ZI. The lowest values were observed in Pergamino and Paraná in 1978, where 55 and 69 % of days with FHB infection events were accompanied by daily values of  $ZI > 0$ , respectively. In other severe epidemics, everywhere there were higher percentages, reaching highs ranging from 92 % in Pergamino in 1985, to 93 % in 2001 in Paraná, up to 100 % of the days in 2001 and 2004 in Balcarce. Figure 13.3 show the 6 day-sequence (2 October to 7 October) of anomaly maps of geopotential height at the level of 1,000 hPa, along the blocking action situation at 70°W observed in 1978. Throughout the period under the influence of this blocking action anticyclone (plus 8 October), 96 % of the total cumulative *Fusarium* index was estimated in Paraná for the wheat campaign of 1978.

### ***13.3.3 Development of Specific Fusarium Head Blight Seasonal Forecasts Based on Hemispheric-Scale Meteorological Predictors***

The atmospheric conditions present irregular fluctuations on wide range of time scales, from weekly to greater scales causing intraseasonal (26–60 days), interannual and interdecadal variability (Garreaud et al. 2008). El Niño Southern Oscillation (ENSO) constitutes the most important oceanic-atmospheric phenomenon causing interannual climate variability. Walker and Bliss (1932) discovered the existence of an irregular interannual fluctuation called Southern Oscillation (SO), which involves changes in the rainfall and wind over the tropical Pacific and Indian oceans. Bjerknes (1969) associated the SO with fluctuations in the surface temperature of the eastern equatorial Pacific Ocean. ENSO phenomenon recognizes a neutral phase and two extreme phases, El Niño (warm sea surface in the central-eastern equatorial Pacific ocean and pressures greater than average in the Indian Ocean and Australia) and La Niña (processes in the opposite direction than in El Niño years). ENSO affects atmospheric circulation systems located at remote sites on the planet (teleconnections), causing thermal and rainfall anomalies. Zhao and Yao (1989) were able to successfully predict 4 months in advance wheat FHB epidemics in eastern China, measuring the surface temperature in the central Pacific Ocean. This association was explained by the ENSO-induced advance of the summer monsoon on East Asia, increasing rainfall and FHB infection events. In southern Brazil, the increment of spring rains coupled with warm anomalies in the tropical Pacific Ocean, was associated with a higher frequency of FHB outbreaks (Del Ponte et al. 2009). The Southern Annular Mode (SAM) or Antarctic Oscillation constitutes another relevant hemispheric-scale meteorological predictor. SAM is the main mode of variability of the extra-tropical circulation in the Southern Hemisphere and is characterized by zonal-symmetric structures or annular, with geopotential height perturbations of opposite sign in Antarctica and in a surrounding zonal band centered near 45°S latitude. Several studies verified the influence of SAM on precipitation in various regions of the planet (Silvestri and Vera 2003; Reason and Rouault 2005; Gillett et al. 2006; Garreaud et al. 2008). Camilioni et al. (2005) observed an increase in the intensity and frequency of winds from the east, probably associated with the southward shift of the Atlantic Ocean subtropical anticyclone in recent decades. These studies supported the idea of calculating indices that consider the dominant meridional circulation (S-SW or N-NE), in response to the power and relative location of the southern subtropical anticyclones of the Atlantic and Pacific oceans.

The effect of many hemispheric-scale meteorological predictors on the probability of occurrence of wheat FHB incidence levels in the Pampas region was identified and quantified, calculating their Kendall correlation coefficients ( $r_k$ ) and fitting logistic regression models (Moschini 2011). The Pampas region was divided in homogeneous areas in relation to temporal variation (1971–2006) of FHB incidence

values (PI %) estimated by Eq. (13.1) (empirical approach). The probabilities of occurrence of three PI % levels (severe, moderate and light to nil) were related to the following meteorological predictors (monthly up to 6-month mean values), processed previously to the occurrence of the wheat susceptible period for infection: Oceanic El Niño index (OENI: from NOAA-USA: sea surface temperature anomaly in El Niño 3.4 region); Southern Oscillation index (SOI: from NCC-Australia: differences of pressure anomalies between Tahiti and Darwin according to Troup 1965); Southern Annular Mode or Antarctic oscillation (SAM: from NERC-UK: monthly differences between surface pressure anomalies registered at six meteorological stations around 40°S and at six near 65°S, according to Marshall 2003); Meridional geopotential height index (Agph or Dgph: absolute or differences between values of gph at 1,000 hPa) (NCEP/NCAR; Kalnay et al. 1996) registered at 100 and 45°W or 60°W, around 40°S; Zonal index (ZI) using for identifying blocking action situations in 100°, 70° y 40°W; interactive effects among variables (product).

In the north-eastern quadrant of the Pampas region (Fig. 13.1), greater disease levels were expected with greater August SAM values (direct relationship, positive  $r_K$ ) and dominance of meridional north-northeastern atmospheric circulation in September (inverse relationship, negative  $r_K$  for the Dgph variable: gph difference between Pacific and Atlantic anticyclones). The best logistic model (five variables) developed for the northeastern region (Model A, Table 13.1) classified correctly 72 % of total years, including the most severe FHB epidemics (1978, 1985, 1993 and 2001). For the central-eastern region, the five-variable model B (Table 13.1) reached a prediction accuracy of 83 %. In both areas, SOI only participated interacting with other variables. In accordance with these findings, maps made for the spring season by Reboita et al. (2009) showed a negative anomaly of precipitation related to a negative MAS phase for the whole Pampas region and a positive to neutral relationship for the north-eastern regional quadrant. Similarly, Silvestri and Vera (2003) found in the central-northern of the Pampas region significant positive correlations (0.35–0.45) between MAS index and precipitation anomaly values for September-October.

In the southern Pampas region, the MAS-linked index did not emerge as significant predictor, coinciding with the non-significant correlations found by Silvestri and Vera (2003) between MAS and precipitation anomaly for the bi-monthly period November-December. Predictors associated to the occurrence of blocking action situations ( $ZI > 0$ ) in South America in 100°W and 70°W (October), were remarkable. Average ZI values in 100°W in October peaked Kendall correlation coefficient ( $r_K = 0.49$ ). The best logistic models (Model C and D, Table 13.1) adjusted for the southern Pampas region, classified satisfactorily the most severe FHB epidemics (1976, 1977, 1985 and 2001), reaching prediction accuracies of 89 and 83 % respectively. In the southern, SOI made a significant contribution to explain the variability in disease levels. When ENSO phenomenon reaches its peak (November-December), wheat heads are in full anthesis (November; more susceptible for FHB infections), unlike northern locations (much earlier anthesis

**Table 13.1** Logistic models fitted in four homogeneous areas (NE: model A; central-E: model B; S-SW: model C and SE: model D) of the Pampas region for estimating the probabilities of occurrence of severe (*Sv*), moderate (*M*) and light to nil (*L*) epidemics, based on hemispheric-scale meteorological predictors. *PA* prediction accuracy

	Model equations <sup>a</sup>	PA %
<b>A</b>	$LogitPrSv = -14.79 + 0.76 SAMa + 0.09 Agph1s - 0.104 Dgph2s - 0.001 It1 - 0.015 It2$ $LogitPrMc = -12.25 + 0.76 MASa + 0.09 Agph1s - 0.104 Dgph2s - 0.001 It1 - 0.015 It2$	72
<b>B</b>	$LogitPrSv = -2.04 + 0.75 SAMa - 0.08 Dgph2s - 0.11 ZI7015s - 0.006 It3 + 0.0013 It4$ $LogitPrMc = -0.0024 + 0.75 SAMa - 0.08 Dgph2s - 0.11 ZI7015s - 0.006 It3 + 0.0013 It4$	83
<b>C</b>	$LogitPrSv = -4.12 - 0.54 SOImjj + 0.44 SOIjas + 0.155 ZI10030o$ $LogitPrMc = -2.31 - 0.54 SOImjj + 0.44 SOIjas + 0.155 ZI10030o$	89
<b>D</b>	$LogitPrSv = -1.96 + 0.15 ZI7030o + 0.18 ZI10030o + 0.015 It5$ $LogitPrMc = 0.29 + 0.15 ZI7030o + 0.18 ZI10030o + 0.015 It5$	83

<sup>a</sup>LogitPrSv = ln(PrSv/1-PrSv); LogitPrMc = ln(PrMc/1-PrMc). Solving the expressions Exp (LogitPrSv)/[1+Exp (LogitPrSv)] and Exp(LogitPrMc)/[1+Exp (LogitPrMc)], PrSv values (probability of observing a severe epidemic (*Sv*) and PrMc (cumulative probability of observing an epidemic => to moderate (*M*)). Ln: natural logarithm. PrM=PrMc-PrSv. PrL=1-(PrSv+PrM), being PrL the probability of observing a light to nil epidemic (*L*). *SAMa*: average value of the Southern Annular Mode (*SAM*) for August. *Agph1s*: September (*s*) value of 1,000 hPa geopotential height (*gph*) in the point 40°S–100°W. *Dgph2s*: difference between September values of 1,000 hPa *gph* of the points 40°S–100°W and 40°S–60°W. *It1*=*Dgph1a*\**Dgph2s*, being *Dgph1a*: difference between August values of 1,000 hPa *gph* of the points 40°S–100°W and 40°S–45°W; *It2*=*Dgph1s*\**SAMja*; being *Dgph1s*: difference between September values of 1,000 hPa *gph* of the points 40°S–100°W and 40°S–45°W and *SAMja*: average value of the *SAM* for July–August.; *It3*=*Dgph2s*\**SOIa*, being *SOIa* the Southern Oscillation index (*SOI*) for August; *It4*=*Dgph2s*\**ZI7015s*, being *ZI7015s*: average of the first September 15-d zonal index values calculated at 70°W by  $ZI = U_{30^{\circ}S} + U_{60^{\circ}S} - 2 U_{45^{\circ}S}$  (*U*: zonal wind at 500 hPa). *SOImjj* and *SOIjas*: average values of the *SOI* for May–June–July and July–August–September respectively. *ZI10030o*; *ZI7030o*: average of the first October 30-d zonal index values calculated at 100°W and at 70°W by *ZI* equation, respectively. *IT5*=*SOIas*\**ZI10030o*, being *SOIas*: average values of the *SOI* for August–September

stage). In accordance, the probability of occurrence of dry periods (derived from conditional probabilities of rain: first order Markov chains and seasonal trend) was up to 30 % lower in El Niño years than in those with La Niña episodes, concentrating this difference in late spring (Moschini et al. 1997). In the same sense, Tanco and Berri (1996) reported that in November–December more than 60 % of the Pampas region registered rainfalls below normal in years with La Niña events. Consistent with these results, Grimm et al. (2000) showed that during the late winter (trimester August–October) precipitation coincided with the median in the central-northern Pampas region for years with El Niño phase, unlike southern regional areas with above-median precipitation in the spring trimester (October–December).

### 13.3.4 Assessing Climate Change Impacts on Fusarium Head Blight

Currently, one of the major challenges is to predict the variations in plant pathosystems in response to anthropogenic greenhouse gas-induced climate change. Assessing the most likely climate change impacts on pathosystems can be made by a retrospective analysis, which identify fingerprints related to climate change in long-term disease observations, or by using mathematical or statistical models. Time series containing standardized disease records are unavailable for the majority of pathogens. In case of having, trends are confounded by changes in management and biological factors over time. When using predictive disease models, major constraints are originated in the uncertainty of the input variables (general circulation climate model-based), the difficulty in estimating biological responses in the presence of nonlinearities and thresholds and the high probability of host-pathogen genetic adaptation to man-induced atmospheric change (Scherin 2004).

Keeping the previous constraints in mind, retrospective and prospective studies were undertaken to analyze climate change effect on wheat FHB in the Pampas region. For both approaches, FHB incidence values were estimated by a simple weather-based model (Eq. 13.2:  $PI \% = -9.15 + 6.47 ND + 0.35 pDD$ , being ND: number of days with simultaneous occurrence of Pr and thermal amplitude  $<7^{\circ}\text{C}$ ; pDD: results of accumulating residuals  $>9^{\circ}\text{C}$  in nT, in those days where xT and nT are  $<25^{\circ}\text{C}$  and  $\geq 9^{\circ}\text{C}$ , respectively). Long-term retrospective FHB incidence predictions (1931–2010) and weather variable (ND and pDD) values were analyzed for Paraná (western Entre Rios province), Pergamino (northern-eastern Buenos Aires province) and Mar del Plata (southern Buenos Aires province). According to Fig. 13.4, the trend lines showed a light increase of FHB incidence over time, with positive slopes larger towards southern Pampas region (Paraná: 0.08 %, Pergamino: 0.16 % and Mar del Plata: 0.24 % per year). In accordance, the largest slope of the trend lines fitted to the variable ND was presented by Mar del Plata (0.031), comparing with Pergamino (0.019) and Paraná (0.006). The trend lines for the thermal variable (pDD) showed positive slopes, being Parana the site with the maximum slope. As it was concluded earlier, in the southern Pampas region (Mar del Plata) 67 and 75 % of years with El Niño and La Niña episodes observed predicted FHB incidence values above and below median, respectively. ENSO phenomenon influence was gradually less clear towards the northern. It is worth pointing out the decline of the FHB incidence levels in the last 9 years, which could indicate that the climate system is still in transition to a new equilibrium, driven by anthropogenic changes in radiative forcing.

Climate change impact on FHB in the Pampas region was also assessed following a prospective approach. FHB incidence values were estimated by Eq. (13.2) using meteorological data from the future (2071–2100), predicted by PRECIS (Providing Regional Climates for Impact Studies) under the medium emission SRES IPCC A2 scenario (Marengo et al. 2009), and from the baseline climate (1961–1990). The anomaly map (future – baseline climate) (Fig. 13.5) showed positive values in southern Buenos Aires province, suggesting an increase in the number of years with moderate to severe FHB incidence under the future climate scenario.

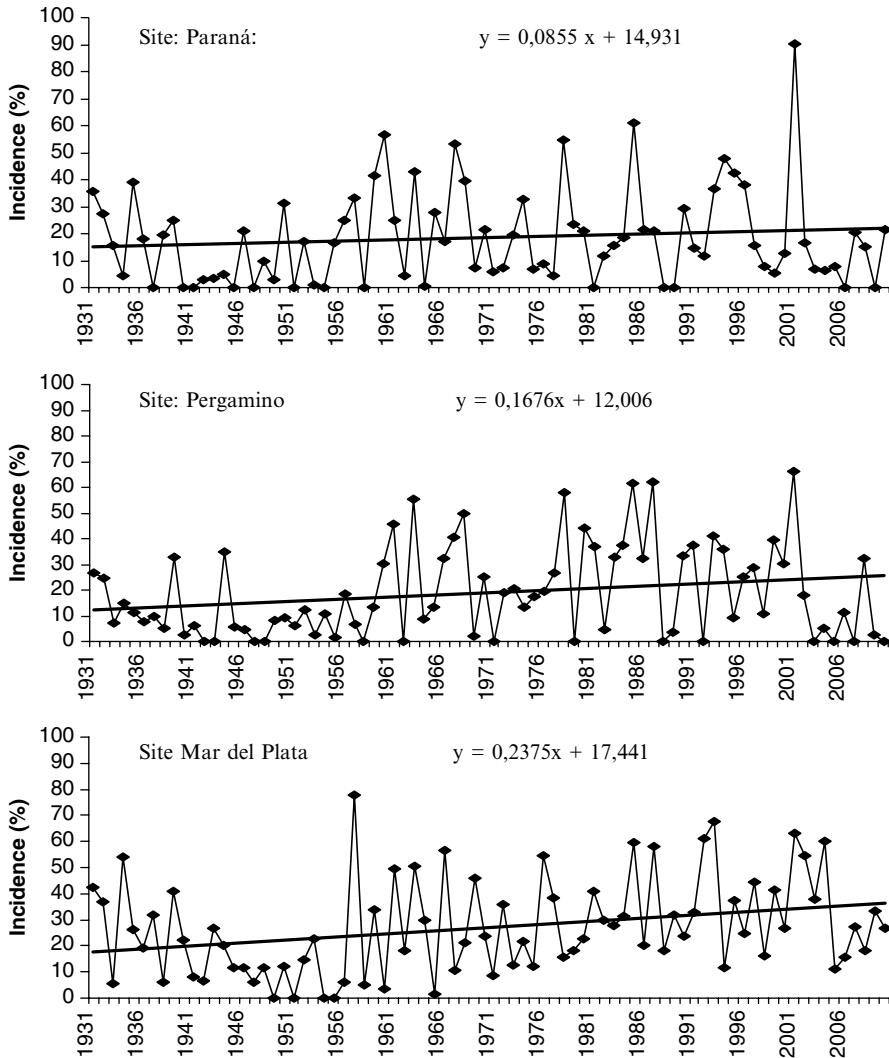
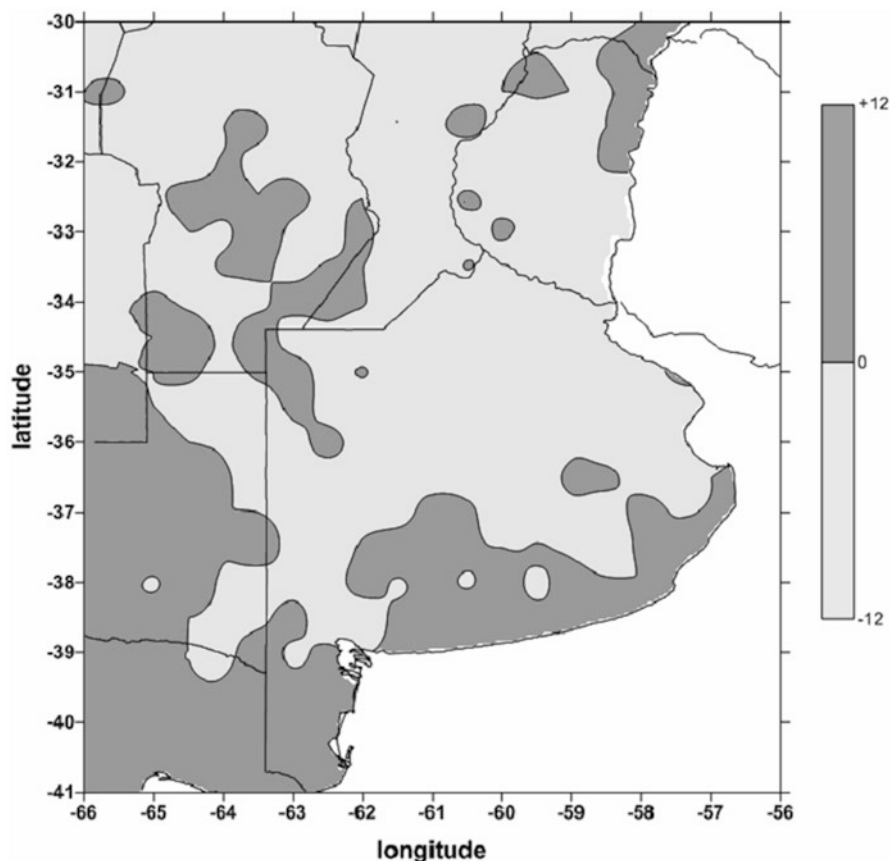


Fig. 13.4 Trend lines of FHB incidence values estimated by Eq. (13.2) (1931–2010) in three sites of the Pampas region

### 13.3.5 Assessing *Fusarium* Head Blight Risk in the Pampas Region

Multiple inoculation episodes in areas with moderate and severe outbreaks suggest that multiple infections contribute to cumulative head blight severity. This fact affects prophylactic disease management options (Francl et al. 1999). There is no



**Fig. 13.5** Anomaly map: difference between the number of years with moderate or severe predicted FHB incidence (Eq. 13.2) using future data (2071–2100) and recent past weather data (1961–1990), in the Pampas region

effective fungicide treatment once the wheat head is infected and colonized. Fungicides with *Fusarium* active ingredients, such as the triazoles, are recommended to be applied prior to infection (preventive treatment) or at maximum 1–2 day post-infection (Annone 2003).

The weather-based model (Eq. 13.1) for predicting FHB incidence has limitations in establishing the stepwise evolution of the epidemic and evaluating the intensity of each infection event. Its meteorological variables are calculated after finishing the entire wheat susceptible period for infection, when the impact of having the estimated disease incidence is not useful for making chemical control decisions. However, González Montaner (2004) explained (southern Pampas region) that disease control decisions are taken when at least two FHB infection periods (defined by the variable  $NP$  of Eq. 13.1) are detected, complemented by the occurrence of

average relative humidity above 70 and 80 % in the 10 days prior to anthesis, for durum and bread wheat respectively. Similarly, Mazzilli et al. (2011) concluded in Uruguay that at least two infection periods (variable *NP*) are needed for FHB epidemics. Following the criterion of no fungicide sprays until two infections events occur, chemical control was avoided in 22 out of 28 flowering dates analyzed (2003–2006), with infection levels similar to those wheat samples sprayed with fungicide at early flowering.

Conclusions derived from the fundamental-empirical FHB forecasting system can be used to assist producers in disease control measures to be employed. From the start of the wheat susceptible period for infection (onset of wheat heading), weather monitoring can detect each FHB infection event and the corresponding predicted FHB index values, in order to make fungicide spray decisions. Since 2005–2006 wheat growing season, a system for assessing FHB risk was implemented for the Pampas region (divided in three sub-regions: northern, central and southern). The system, three times a week (Monday, Wednesday and Friday), updates daily meteorological data from 45 standard weather stations for running predictive FHB models (empirical and fundamental-empirical approaches). Also, a specific short range weather forecast is elaborated. After analyzing all together (weather forecast and disease model outputs), comments and maps showing the spatial distribution of the three possible FHB risk grades (severe: red, moderate: yellow and/or light: green), are presented at the web page: <http://climayagua.inta.gob.ar>

### ***13.3.6 Estimating Spatial Distribution of Fusarium Head Blight Incidence Using Land and Remote Sensing Data***

Disease estimates from weather-based models are usually reduced to punctual data because weather station data are used as inputs. To generate disease maps, these results need to be taken to an extensive area through interpolation methodologies. As a consequence, estimated values in sites where weather station data are not available contain additional uncertainties. This is clearly observed in areas where weather station network is sparse and irregularly distributed (Solis Villagran and Flores Garnica 2003). Hence, the inclusion of remote sensing data into disease models could be a solution. Remote sensing is a multiple purpose tool with many important specific applications such as regional estimation of precipitation amount/occurrence and surface temperature, evaluation of natural resources and land cover classification (Fattorelli et al. 1995).

In order to improve the estimated spatial distribution of FHB incidence in the Pampas region, Sepulcri (2010) and Sepulcri et al. (2010) included satellite data in the calculation of disease incidence by Eq. (13.1) (empirical approach). The spatial distribution of model-based FHB incidence values using only land weather station network data (Fig. 13.6a) was compared with those using land and satellite data. Firstly, precipitation occurrence data from satellite Tropical Rainfall Measurement Mission (TRMM, 3B42 product), previously tested against pluviometer records

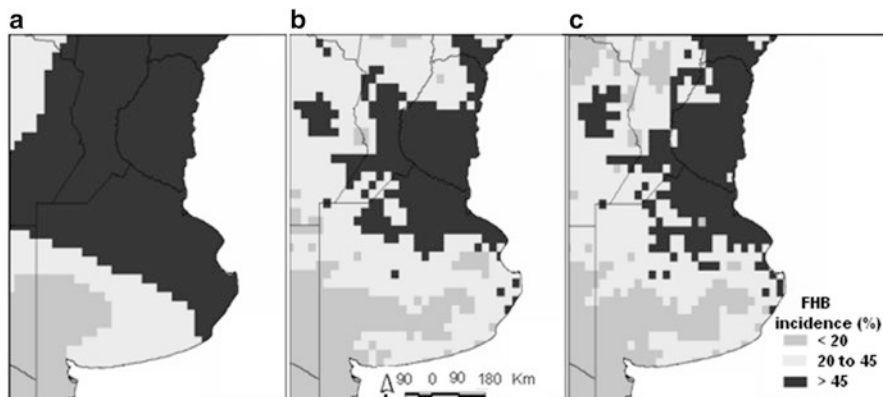


**Fig. 13.6** Spatial distribution of FHB incidence values estimated by Eq. (13.1) (classified in percentage categories: >45 %, 20–45 % and <20 %), using only land weather station network data (a), land and precipitation satellite data (b) and land and precipitation-temperature satellite data (c) for 2001 wheat growing season (mean heading date)

(85 % accuracy), combined with interpolated temperature and relative humidity weather station data were used for estimating FHB incidence by Eq. (13.1) (Fig. 13.6b). The product 3B42 provides precipitation estimations every 3 h with a spatial resolution of  $0.25^\circ$ , for all the longitudinal range and from  $50^\circ\text{N}$  to  $50^\circ\text{S}$  latitude (Huffman et al. 2007). Secondly, it was added temperature data obtained from a climatic zoning based on NOAA-AVHRR images, together with satellite (TRMM) precipitation estimates and interpolated relative humidity station data (Fig. 13.6c). Evaluations with field data suggested that when the Eq. (13.1) used satellite data, FHB incidence was represented in a reliable way, mainly in data-sparse areas.

## 13.4 Conclusions

From simple daily meteorological elements (maximum and minimum temperatures, precipitation and relative humidity), FHB intensity and grain DON content values can be satisfactorily estimated by forecasting systems (empirical and fundamental-empirical approaches) developed/validated in the Pampas region. Retrospective and real time model outputs were crucial to address many applications, previously described.

Nevertheless, due to the inherent variability accompanying the precise definition of each disease pyramid component, it should be noted the lack of mathematical precision in the estimates of the disease forecasting systems. In relation to the pathometry, it was often found that FHB incidence values observed from samples collected from a particular field crop presented high variability, complicating their contrasts with predicted values. Also in already cited controlled environment

studies with artificial inoculation, it was pointed out that local *Fusarium* strains showed greater aggressiveness and adaptation to lower temperatures (Zoldan 2008; Martinez et al. 2012) than the strain used by Andersen (1948). In respect to the host, McMullen et al. (1997) indicated that wheat is susceptible to disease from anthesis until soft dough stage. This susceptible period for infection is highly variable among wheat cultivars, due to head characteristics, and years, in response to prevailing weather conditions. De Souza and Formento (2004) and Reis (1989) described different field crop anthesis progress curves in Paraná (Pampas region) and Passo Fundo (southern Brazil), responding to the wheat cultivar-environment interactive system. From this fact, inaccuracies in model-based predictions (fundamental-empirical approach) may be inferred because a unique model was fitted to the anthesis progress curve observed in a particular wheat cultivar and one growing season. Finally, weather-based forecasting systems were developed under the assumption of non-limiting inoculum and lack of response to crop rotation, due to the marked ubiquity of *Fusarium* species, wide range of hosts and high anemophilous spore dissemination (Reis and Carmona 2002). It was also assumed that the effects of wheat cultivar behavior regarding the disease and cultural practices such as tillage systems do not play a significant role for explaining the observed disease variability (Schaafsma et al. 2001; Lori et al. 2009).

## References

- Alessandro AP (2003) The influence of blocking events on temperature and precipitation in Argentina during the 1990s. *Meteorológica* 28(1 y 2):39–52
- Andersen AL (1948) The development of *Gibberella zeae* head blight of wheat. *Phytopathology* 38:599–611
- Annone JG (2003) Particularidades del control químico de la FET. Seminario: problemas asociados a la Fusariosis en trigo y estrategias para su prevención. Bolsa de Cereales de Buenos Aires, Argentina
- Baker KM, Kirk WW (2007) Comparative analysis of models integrating synoptic forecast data into potato late blight risk estimate systems. *Comput Electron Agric* 57:23–32
- Bjerknes J (1969) Atmospheric teleconnections from the equatorial Pacific. *Mon Weather Rev* 97:163–172
- Bourke PMA (1970) Use of weather information in the prediction of plant disease epiphytotics. *Annu Rev Phytopathol* 8:345–370
- Camilioni I, Barros V, Escobar G, Di Luca A (2005) Tendencias en la posición del Anticiclón del Atlántico Sur y su representación por modelos climáticos globales: impactos sobre el estuario del Río de la Plata y océano adyacente. IX Congreso Argentina de Meteorología Buenos Aires Argentina
- Carranza MR, Lori GA, Sisterna MN (2002) Fusaria involved in the head blight complex of wheat in Argentina. *Fitopatología* 37:164–168
- Carranza MR, Moschini RC, Kraan G, Bariffi JH (2007) Examination of meteorology-based predictions of Fusarium head blight of wheat grown at two locations in the southern Pampas region of Argentina. *Aust Plant Pathol* 36:305–308
- De Souza J, Formento N (2004) Estudios de antesis en trigo y su relación con la Fusariosis (*Fusarium graminearum* y *Fusarium* spp.) VI Congreso Nacional de Trigo. Bahía Blanca Argentina

- Del Ponte EM, Fernandes JMC, Pavan WA, Baethgen WE (2009) A model-based assessment of the impacts of climate variability on Fusarium Head Blight seasonal risk in southern Brazil. *J Phytopathol* 157:675–681
- Faifer GC, Zabal O, Godoy HM (1992) Further studies on the hematopoietic damage produced by a single dose of T-2 toxin in mice. *Toxicology* 75:169–174
- Fattorelli S, Casale R, Borga M, Da Ros D (1995) Integrating radar and remote sensing techniques of rainfall estimation in hydrological applications for flood hazard mitigation. The European contribution: perspectives and prospects. Rue de la Loi B-1049, Brussels, Bélgica
- Franc L, Shaner G, Bergstrom G, Gilbert J, Pedersen W, Dill-Macky R, Sweets L, Corwin B, Jin Y, Gallenberg D, Wiersma J (1999) Daily inoculum levels of *Gibberella zeae* on wheat spikes. *Plant Dis* 83:622–666
- Garreaud RD, Vuille M, Compagnucci R, Marengo J (2008) Present-day South American climate. *PALAEO3 Spec Issue (LOTRED South America)* 281:180–195. doi:10.1016/j.palaeo.2007.10.032
- Gillett NP, Kell TD, Jones PD (2006) Regional climate impacts of the Southern Annular Mode. *Geophys Res Lett*:L23704. doi:10.1029/2006GL027721
- González MJ (2004) Avances en el control de enfermedades en trigo. A Todo Trigo, un Congreso para todos Mar del Plata, Argentina, pp 43–54
- Grimm AM, Barros VR, Doyle ME (2000) Climate variability in southern South America associated with El Niño and La Niña events. *J Clim* 13:35–58
- Hooker DC, Shaafsma AW, Tamburic-Ilincic L (2002) Using weather variables pre-and post-heading to predict deoxynivalenol content in winter wheat. *Plant Dis* 86:611–619
- Huffman GJ, Adler RF, Bolvin DT, Gu G, Nelkin EJ, Bowman KP, Hong Y, Stocker EF, Wolff DB (2007) The TRMM Multisatellite precipitation analysis (TMPA): quasi-global, multiyear, combined-sensor precipitation estimates at fine scales. *J Hydrometeorol* 8:38–55
- Kalnay EM, Kanamitsu M, Kistler R, Collins W, Deaven D, Gandia L, Iredell M, Saha S, White G, Woollen J, Zhu Y, Chelliah M, Ebisuzaki W, Higgins W, Janowiak J, Mo KC, Ropelewski C, Wang J, Leetmaa A, Reynolds R, Jenne R, Joseph D (1996) The NCEP/NCAR 40 year reanalysis project. *Bull Am Meteorol Soc* 77:437–471
- Lacey J, Bateman GL, Mirocha CJ (1999) Effects of infection time and moisture on development of ear blight and deoxynivalenol production by *Fusarium* spp. in wheat. *Ann Appl Biol* 134:277–283
- Lori GA, Sisterna MN, Sarandón SJ, Rizzo I, Chidichimo H (2009) Fusarium head blight in wheat: impact of tillage and other agronomic practices under natural infection. *Crop Prot* 28:495–502
- Lund IA (1963) Map pattern classification by statistical methods. *J Appl Meteorol* 2:56–65
- Marengo JA, Jones R, Alves LM, Muniz L, Valverde M (2009) Future change of temperature and precipitation extremes in South America as derived from PRECIS regional climate modeling system. *Int J Climatol*. doi:10.1002/joc.1863
- Marshall GJ (2003) Trends in the Southern annular mode from observations and reanalyses. *J Clim* 16:4134–4143
- Martínez MI, Moschini RC, Barreto D, Comerio R (2012) Effect of environment on Fusarium head blight intensity and deoxynivalenol content in wheat grains: development of a forecasting system. *Cereal Res Commun* 40:74–84
- Mazzilli S, Pérez C, Ernst O (2011) Una alternativa para optimizar el uso de fungicidas para controlar fusariosis de espiga en trigo. *Agrociencia* 15:60–68
- McMullen M, Jones R, Gallegberg D (1997) Scab of wheat and barley: a re-emerging disease of devastating impact. *Plant Dis* 81:1340–1348
- Moschini RC (2011) Desarrollo y uso de sistemas de pronóstico de epidemias de la Fusariosis de la Espiga de Trigo (*Triticum aestivum* L.) para identificar situaciones sinópticas y predictores meteorológicos en diferentes escalas asociados a la enfermedad en la región pampeana. Tesis Doctorado Universidad de Buenos Aires, Argentina

- Moschini RC, Fortugno C (1996) Predicting wheat head blight incidence using models based on meteorological factors in Pergamino, Argentina. *Eur J Plant Pathol* 102:211–218
- Moschini RC, Casagrande G, Vergara G, Conti HA (1997) Efectos del ENSO sobre las probabilidades de períodos secos derivadas de modelos markovianos de primer orden, en La Pampa. *Rev Facultad de Agronomía* 17:71–76
- Moschini RC, Pioli R, Carmona MA, Sacchi O (2001) Empirical predictions of wheat head blight in the northern Argentinean Pampas region. *Crop Sci* 41:1541–1545
- Moschini RC, de Galich MTV, Annone JG, Polidoro O (2002) Enfoque Fundamental-Empírico para estimar la evolución del Índice de *Fusarium* en trigo. *RIA* 31:39–53
- Moschini RC, Carranza MR, Carmona M (2004) Meteorological-based predictions of wheat head blight epidemic in the southern Argentinean pampas region. *Cereal Res Commun* 32:45–52
- Moschini RC, Bischoff S, Martínez MI (2008) Variabilidad climática y enfermedades. Caso de estudio: Fusariosis de la espiga de trigo. *Horizonte A. Magazine de las Ciencias Agrarias*. Año 5(21):10–15
- Moschini RC, Castellarín JM, Martínez MI, Ferraguti F (2012) Análisis de la Fusariosis de la espiga de trigo en Oliveros en la campaña 2011/12. Sistemas de pronóstico basados en variables meteorológicas para estimar su distribución anual y el riesgo climático en la región pampeana. Serie Para Mejorar la Producción. Cultivos Invernales (47) EEA Oliveros, pp 49–54
- Paul PA, Lipps PE, Madden LV (2005) Relationship between visual estimates of *Fusarium* head blight intensity and deoxynivalenol content in harvest wheat grain: a meta-analysis. *Phytopathology* 95:1225–1236
- Raposo R, Wilks DS, Fry WE (1993) Evaluation of potato late blight forecasts modified to include weather forecasts: a simulation analysis. *Phytopathology* 83:103–108
- Reason CJC, Rouault M (2005) Links between the Antarctic oscillation and winter rainfall over western South Africa. *Geophys Res Lett* 32, L07705. doi:[10.1029/2005GL022419](https://doi.org/10.1029/2005GL022419)
- Reboita MS, Ambrizzi T, Da Rocha RP (2009) Relationship between the southern annular mode and southern hemisphere atmospheric systems. *Rev Bras Meteorol* 24:48–55
- Reis EM (1989) Fusariosis: biología y epidemiología de *Gibberella zae* en trigo. In: Kholi M (ed) Taller sobre Fusariosis de la espiga en América del Sur. CIMMYT, Mexico, pp 97–102
- Reis EM, Carmona M (2002) Fusariosis del trigo. Biología, epidemiología y estrategias para su manejo, 1ª Edición. Buenos Aires, p 25. ISBN: 98743–3959
- Scherm H (2004) Climate change: can we predict the impacts on plant pathology and pest management? *Can J Plant Pathol* 26:267–273
- Sepulcri G (2010) Predicción de la Fusariosis de la espiga de trigo a partir de modelos que incorporan información satelital. Tesis Magister área Producción Vegetal, Universidad de Buenos Aires, Argentina
- Sepulcri G, Moschini RC, Di Bella CM (2010) Estimación de Fusariosis incorporando información satelital. *Horizonte A. Magazine de las Ciencias Agrarias*. Año 6(30):32–33
- Shaafsma AW, Tamburic-Ilinic L, Millar JD, Hooker DC (2001) Agronomic consideration for reducing DON in wheat grain. *Can J Plant Pathol* 23:279–285
- Silvestri GE, Vera CS (2003) Antarctic Oscillation signal on precipitation anomalies over southeastern South America. *Geophys Res Lett*. doi:[10.1029/2003GL018277](https://doi.org/10.1029/2003GL018277)
- Snijders CHA, Krechting CF (1992) Inhibition of deoxynivalenol translocation and fungal colonization in *Fusarium* head blight resistant wheat. *Can J Bot* 70:1570–1576
- Solis VZ, Flores GJG (2003) Análisis comparativo de técnicas de interpolación en la estimación de la variación espacial de factores en una cuenca hidrográfica. XIII Reunión Nacional SELPER Puerto Vallarta México DF
- Tanco R, Berri GJ (1996) Acerca del efecto del fenómeno El Niño sobre la precipitación en la Pampa Húmeda Argentina. *Actas del VII Congreso Argentino y VII Congreso Latinoamericano e Ibérico de Meteorología Bs As Argentina*
- Vincelli PC, Lorbeer JW (1988) Relationship of precipitation probability to infection potential of *Botrytis squamosa* on onion. *Phytopathology* 78:1078–1082
- Walker GT, Bliss EW (1932) World weather V Mem. Royal Meteor Soc 4:53–84

- Xu XM, Monger W, Ritieni A, Nicholson P (2007) Effect of temperature and duration of wetness during initial infection periods on disease development, fungal biomass and mycotoxin concentrations on wheat inoculated with single, or combinations of *Fusarium* species. *Plant Pathol* 56:943–956
- Zhao S, Yao C (1989) On the sea temperature prediction models of the prevailing level of wheat scab. *Acta Phytopathol Sin* 19:229–234
- Zoldan SM (2008) Regioes de risco, caracterizacao da antese em cereais de inverno e sistema de alerta para a Giberela, em trigo. Tesis Doctor en Agronomía área de Fitopatología, Universidad de PassoFundo, Brazil